Neuron, Vol. 30, 475–488, May, 2001, Copyright ©2001 by Cell Press

# *Drosophila* Hsc70-4 Is Critical for Neurotransmitter Exocytosis In Vivo

**Peter Bronk,[1] Julia J. Wenniger,[1] Ken Dawson-Scully,[2] Xiufang Guo,[1] Susie Hong,[1] Harold L. Atwood,[2] and Konrad E. Zinsmaier[1,3]**
[1]Department of Neuroscience
234d Stemmler Hall
University of Pennsylvania School of Medicine
Philadelphia, Pennsylvania 19104
[2]Department of Physiology
Medical Science Building
University of Toronto
Toronto, Ontario M5S 1A8
Canada

## Summary

**Previous in vitro studies of cysteine-string protein (CSP) imply a potential role for the clathrin-uncoating ATPase Hsc70 in exocytosis. We show that hypomorphic mutations in *Drosophila* Hsc70-4 (Hsc4) impair nerve-evoked neurotransmitter release, but not synaptic vesicle recycling in vivo. The loss of release can be restored by increasing external or internal $Ca^{2+}$ and is caused by a reduced $Ca^{2+}$ sensitivity of exocytosis downstream of $Ca^{2+}$ entry. Hsc4 and CSP are likely to act in common pathways, as indicated by their in vitro protein interaction, the similar loss of evoked release in individual and double mutants, and genetic interactions causing a loss of release in trans-heterozygous *hsc4-csp* double mutants. We suggest that Hsc4 and CSP cooperatively augment the probability of release by increasing the $Ca^{2+}$ sensitivity of vesicle fusion.**

## Introduction

Regulated neurotransmitter release is accomplished by coupling nerve activity and exocytosis on a submillisecond scale, such that $Ca^{2+}$ influx through $Ca^{2+}$ channels triggers the fusion of synaptic vesicles with the presynaptic plasma membrane. Membrane fusion is in part mediated by the SNARE or core complex including the proteins synaptobrevin, syntaxin, and SNAP-25 (Benfenati et al., 1999). After exocytosis, vesicle membranes and most of their unique proteins are rapidly recaptured and locally recycled by at least two kinetically distinct endocytotic pathways, the "kiss and run" pathway (Ceccarelli et al., 1973), and receptor-mediated endocytosis (Heuser and Reese, 1973).

The 70 kDa heat-shock cognate protein (Hsc70) catalyzes in vitro and in vivo the uncoating of clathrin-coated vesicles, the final step of receptor-mediated endocytosis (Rothman and Schmid, 1986; Cremona and De Camilli, 1997; Newmyer and Schmid, 2001). Hsc70 is a constitutively expressed member of the stress-induced Hsp70 family, which exhibits a weak intrinsic ATPase activity that is significantly stimulated by its binding to cofactors (Bukau and Horwich, 1998). Hsc70-dependent clathrin coat dissociation is catalyzed by the cofactor auxilin (Ungewickell et al., 1995). In vitro, auxilin recruits Hsc70 via its J-domain to an auxilin-Hsc70-clathrin lattice complex, and stimulates Hsc70-mediated ATP hydrolysis inducing the release of clathrin triskelions from the clathrin lattice (Ungewickell et al., 1995). Consistently, loss of auxilin in *C. elegans* impairs clathrin-mediated endocytosis and arrests development (Greener et al., 2001). In addition to clathrin-uncoating, Hsc70 may also chaperone clathrin triskelions after coat dissociation, preventing inappropriate cytosolic polymerization of clathrin, and may prime clathrin triskelions to reform clathrin-coated pits (Jiang et al., 2000).

Independent studies of cysteine-string protein (CSP) raised the possibility that Hsc70 might also mediate steps of neurotransmitter exocytosis. CSP is associated with secretory vesicles and contains a J-domain similar to that of auxilin (Chamberlain and Burgoyne, 2000). The J-domain of CSP is essential and sufficient to bind Hsc70 and to stimulate its intrinsic ATPase activity in vitro, suggesting that CSP could act as a critical cofactor of Hsc70 (Braun et al., 1996; Chamberlain and Burgoyne, 1997). Studies of *csp* null mutations in *Drosophila* demonstrated a critical role for CSP in regulated neurotransmitter exocytosis (Umbach et al., 1994; Zinsmaier et al., 1994; Dawson-Scully et al., 2000), but not in synaptic vesicle recycling (Ranjan et al., 1998). Accordingly, CSP might recruit Hsc70 to synaptic vesicles facilitating a step of exocytosis in a manner similar to the auxilin-mediated recruitment of Hsc70 in endocytosis. However, no in vivo evidence for such a role in exocytosis has been reported so far.

To test the proposed in vivo role of Hsc70 in exocytosis, we generated a series of mutations in *Drosophila* Hsc4, the closest homologue of bovine Hsc70, and examined their effects on the physiology of larval neuromuscular junctions (NMJs). Stimulus-evoked synaptic transmission elicited at 0.2 Hz in hypomorphic *hsc4* mutants was reduced by ~50% at 23°C, and abolished above 30°C. The defect was intrinsic to the presynaptic terminal, because neither nerve excitation, nor the postsynaptic sensitivity to neurotransmitter was impaired. Further experiments localized the defect to a step that is likely to increase the $Ca^{2+}$ sensitivity of $Ca^{2+}$-triggered vesicle fusion downstream of the $Ca^{2+}$ sensor. In addition, a thermo-intolerant defect of $Ca^{2+}$ clearance was indicated by increased $Ca^{2+}$ resting levels in presynaptic terminals at 34°C. The thermo-intolerant loss and the reduced $Ca^{2+}$ sensitivity of exocytosis in *hsc4* mutants are reminiscent of the defects observed in *Drosophila csp* mutants. Because homozygous *hsc4-csp* double mutants showed a similar loss of evoked release as individual *csp* and *hsc4* mutants, it appeared likely that both proteins act in the same signaling pathway. This idea was strengthened by the ATP-dependent interaction of Hsc4 with CSP in vitro, and in vivo by genetic interactions causing a loss of evoked release in trans-heterozygous *hsc4-csp* double mutants.

[3]Correspondence: zinsmaie@mail.med.upenn.edu

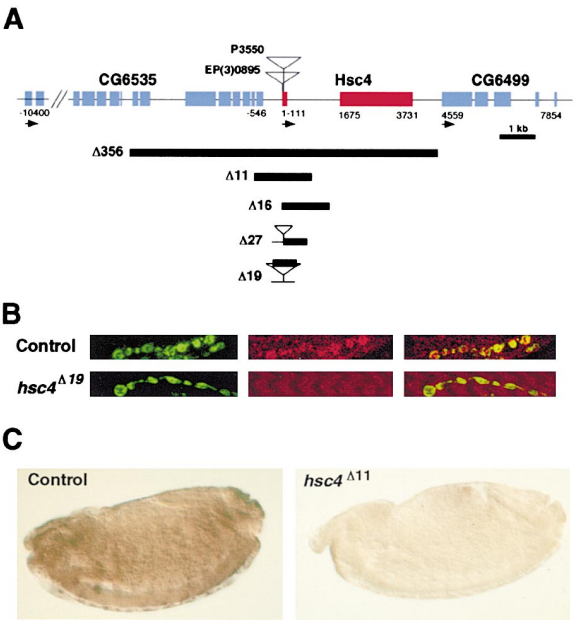


Figure 1. Mutations in the *Drosophila hsc4* Gene

(A) Genomic map of the *hsc4* gene. Red boxes indicate exons of the *hsc4* gene; blue boxes indicate putative exons of the neighboring genes *CG6535* and *CG6499*, which were predicted by the Fly Genome Project from the genomic sequence AE003708 (Adams et al., 2000). Number 1 of the depicted sequence indicates the start site of Hsc4 transcription after Perkins et al. (1990). Arrows below indicate direction of transcription. P element insertion sites (triangles) and DNA deletions (black bars) are indicated. The Δ*356* deletion spans from −4357 to 4416, Δ*11* from −813 to 853, Δ*16* from 1 to 1369, and Δ*27* from 1 to 698. Δ*27* also contains a 611 bp insertion derived from the original P insert. The P insertion Δ*19* contains a large internal deletion within the original P element insertion but normal flanking genomic sequences.

(B) Double-immunostaining of 3rd instar larval NMJs in control and homozygous $hsc4^{\Delta 19}$ mutants with antibodies against CSP (green, left panel) and Hsc4 (red, middle panel). The degree of colocalization is indicated by the overlay (yellow, right panel).

(C) Immunostaining of control and homozygous $hsc4^{\Delta 11}$ mutant embryos (stage 13) with antibodies against Hsc4. Hsc4 is widely expressed in control, but not in $hsc4^{\Delta 11}$ mutant embryos.

## Results

### Null Mutations of *Drosophila* Hsc4 Arrest Development in First Instar Larvae

In *Drosophila*, two heat-inducible (Hsp68 and Hsp70) and five constitutively (Hsc70-1 to Hsc70-5) expressed members of the Hsp70 family have been identified. Hsp68 and Hsp70 are virtually absent under nonstress conditions, while Hsc70-1 and Hsc70-2 expression is only detected late in development during pupal and adult stages (Craig et al., 1983). Hsc70-3 is apparently associated with the lumen of the endoplasmic reticulum, and Hsc70-5 is likely a mitochondrial protein (Rubin et al., 1993). Hsc70-4 (Hsc4) shows the highest sequence homology to bovine Hsc70 and is constitutively expressed throughout development in neurons and nonneuronal cells (Craig et al., 1983; Palter et al., 1986; Perkins et al., 1990). Its strong expression in the garland cells (Perkins et al., 1990), which exhibit a high rate of endocytosis, and its synaptic expression at larval NMJs (Figure 1B) suggest that Hsc4 may have a role similar to bovine Hsc70. Therefore, we mutagenized the *hsc4* gene to test the proposed role of Hsc70 in neurotransmitter exocytosis.

The P element insertions *l(3)3550* and *EP(3)0895* (Hing et al., 1999; Rorth et al., 1998; Spradling et al., 1995) are both semilethal, allowing development of some escapers to adulthood (Table 1). Both transposons are inserted into the first exon of the *hsc4* gene (Figure 1A), just after the proposed RNA-transcription start site (Perkins et al., 1990). To obtain stronger mutations, we remobilized the P element in $hsc4^{3550}$ to generate precise and imprecise excisions. Three additional classes of alleles were recovered (Table 1): recessive lethal alleles causing developmental arrest in early larval stages, recessive lethal alleles interrupting development during late larval to early pupal stages, and viable alleles reverting the semilethal phenotype of the original insertion. Homozygous larvae from all lethal groups showed sporadic but reduced muscle contractions suggestive of a neurological defect. Like $hsc4^{R12}$, all alleles of the viable group were precise excisions, restoring the original gene sequence and thus excluding a second-site mutation.

The lethal mutations $hsc4^{\Delta 11}$, $hsc4^{\Delta 16}$, $hsc4^{\Delta 27}$, and $hsc4^{\Delta 356}$ are likely null alleles causing developmental arrest in homozygous first instar larvae 6–12 hr after hatching from the eggshell. Molecular analysis revealed deletions of the *hsc4* gene in all these alleles (Figure 1A). The largest, $hsc4^{\Delta 356}$, deletes the entire *hsc4* gene, but also parts of the predicted neighboring genes (Adams et al., 2000). The remaining alleles, $hsc4^{\Delta 11}$, $hsc4^{\Delta 16}$, and $hsc4^{\Delta 27}$ delete the promoter and the first exon of the gene. The second class of mutations consists of only one allele, $hsc4^{\Delta 19}$, which arrests development between the larval 3rd instar and an early pupal stage. Because the molecular analysis of $hsc4^{\Delta 19}$ revealed only an internal deletion within the P element, the P insertions in the phenotypically weaker alleles, *EP(3)0895* and *l(3)3550*, may facilitate some expression of Hsc4.

Immunostaining of *hsc4* mutant embryos confirmed a loss of Hsc4 expression in the deletion alleles. Hsc4 immunostaining was virtually absent in homozygous $hsc4^{\Delta 11}$ embryos (Figure 1C) and the other alleles of this group (data not shown). In control embryos, Hsc4 was widely and abundantly expressed, most likely in all embryonic cells as suggested earlier (Palter et al., 1986; Perkins et al., 1990). Hsc4 immunostaining was also not detectable in synaptic boutons of homozygous $hsc4^{\Delta 19}$ 3rd instar larvae (Figure 1B).

### Nerve-Evoked Neurotransmitter Release at *hsc4* Mutant Larval NMJs Is Reduced

We examined synaptic transmission at NMJs of 3rd instar larvae in controls and *hsc4* mutants by recording nerve-evoked excitatory junctional potentials (EJPs) and spontaneous excitatory junctional potentials (mEJPs) from muscle 6 in the presence of 1 mM external $Ca^{2+}$. At 22°C–23°C, nerve-evoked EJP amplitudes recorded from homozygous $hsc4^{\Delta 19}$ NMJs were significantly reduced to 55% ± 6% of control (Figures 2A and 2B). EJP amplitudes were not reduced by a fatigue of evoked release, because responses sequentially recorded at 0.2 Hz did not progressively diminish (Figure 2A). Homozy-

Table 1. Mutations of Hsc4 in *Drosophila*

| hsc4 Allele | Lethal Stage | Mutation | Allele Class |
|---|---|---|---|
| *Δ356* | 1st instar larvae | deletion | 1 |
| *Δ11* | 1st instar larvae | deletion | 1 |
| *Δ16* | 1st instar larvae | deletion | 1 |
| *Δ21* | 1st instar larvae | deletion | 1 |
| *Δ27* | 1st instar larvae | deletion | 1 |
| *Δ19* | late larvae-early pupae | insertion | 2 |
| *l(3)03550* | early pupae-adult | insertion | 3 |
| *EP(3)0859* | early pupae-adult | insertion | 3 |
| *R12* | viable | Revertant of *l(3)3550* | – |
| *P[hsc4]* | viable | genomic *hsc4* transgene | rescue |

The allele *l(3)3550* was originally isolated by Spradling et al. (1995), *EP(3)0859* was isolated by Rorth et al. (1998), and *P[hsc4]* was generated by Hing et al. (1999).

gous $hsc4^{3550}$ mutants and trans-heterozygous combinations of $hsc4^{\Delta 19}$ with $hsc4^{\Delta 11}$ and $hsc4^{\Delta 356}$ showed a statistically similar reduction of EJP amplitudes while those from the precise excision $hsc4^{R12}$ were normal (Figure 2B). One copy of a 14 kb genomic DNA fragment *P[hsc4],* spanning from around position −2,000 to +12,000 (see Figure 1A), rescued the recessive lethality of $hsc4^{3550}$ (Hing et al., 1999) and the loss of synaptic transmission in homozygous $hsc4^{\Delta 19}$ mutants (Figure 2B), correlating the phenotypic effects of the mutations with the *hsc4* gene.

Evoked (Figure 2C), but not spontaneous synaptic transmission (data not shown), was thermo-intolerant in *hsc4* mutants. After increasing the temperature from 23°C to 30°C, homozygous $hsc4^{\Delta 19}$ mutants showed a complete loss of EJP amplitudes after 20 min when stimulated at 0.2 Hz. After cooling to 23°C, at least a partial recovery of EJPs was always observed within 11 min. This thermo-intolerance of evoked neurotransmission indicates that Hsc4 may mediate a thermal protection of synaptic proteins.

The loss of nerve-evoked synaptic transmission in *hsc4* mutants could arise at many different steps, from failure of nerve excitation to loss of postsynaptic glutamate receptor activities. To exclude a failure of nerve excitation or conduction, we electrotouically elicited EJPs in the absence of $Na^+$ channel-mediated action potentials, which were blocked by application of the $Na^+$ channel inhibitor Tetrodotoxin (TTX). Electrotonic stimulation of release is possible by positioning the stimulating electrode close to the nerve terminal and using stimuli with increasing intensity (Yuan and Ganetzky, 1999). At a normal stimulation intensity, application of 5 μM TTX completely abolished nerve-evoked EJPs, both in control and *hsc4* mutants. Subsequent stimulation with intensities 10-fold over threshold then elicited EJPs in control and $hsc4^{\Delta 19}$ mutants (Figure 2D). However, such electrotonically elicited EJPs were still reduced in $hsc4^{\Delta 19}$ to 49% ± 14% of control, thus indicating a defect downstream of nerve excitation.

Analysis of spontaneous neurotransmitter release revealed no postsynaptic defects at *hsc4* mutant NMJs. The cumulative distribution of mEJP amplitudes in homozygous $hsc4^{\Delta 19}$ was similar to control (Figure 2E). Furthermore, the mean amplitude and frequency of spontaneously occurring mEJPs in homozygous $hsc4^{\Delta 19}$ larvae and trans-heterozygous combinations of $hsc4^{\Delta 19}$ with $hsc4^{\Delta 11}$ and $hsc4^{\Delta 356}$ showed no significant differences to control (Figures 2F and 2G). The normal frequency of spontaneously occurring mEJPs is consistent with a normal number of release sites in *hsc4* mutant NMJs. The normal mEJP amplitudes indicate that neither the sensitivity of the postsynaptic muscle to neurotransmitter, nor the amount of transmitter contained in synaptic vesicles is impaired in *hsc4* mutants. Consequently, the loss of evoked neurotransmission must be intrinsic to a mechanism of neurotransmitter release.

The loss of evoked neurotransmitter release in *hsc4* mutants is not caused by a significant defect in neuromuscular development, because immunostaining of NMJs revealed no abnormalities in the gross morphology of $hsc4^{\Delta 19}$ mutant NMJs (Figure 3A). The loss of release was also not due to a reduced expression of various synaptic proteins in mutant boutons (Figure 3B). No significant difference in fluorescence staining intensity was observed for synaptobrevin I, synaptotagmin, syntaxin, CSP, LAP (a AP-180 homolog), and clathrin. Furthermore, no expression differences were found in larval brain extracts of $hsc4^{\Delta 19}$ and controls for all of the examined synaptic proteins (Figure 3C). To test whether the loss of Hsc4 could be in part compensated by an upregulation of related Hsc70 proteins, we examined the expression of stress-induced Hsp70 in *hsc4* mutant 1st instar larvae raised at 18°C. Hsp70 was detectable in protein extracts of $hsc4^{\Delta 11}$ and $hsc4^{\Delta 27}$ mutant extracts, but not in control extracts (Figure 3D). Because the antibody may crossreact with other Hsc70 isoforms, this suggests that Hsp70 or a related Hsc70 homolog could compensate for some of the deficits induced by the loss of Hsc4.

### $Ca^{2+}$ Sensitivity of Evoked Release, but Not $Ca^{2+}$ Cooperativity, Is Impaired in *hsc4* Mutants

To quantify the reduction in neurotransmitter release, we estimated the number of quanta released per stimulus as defined by the ratio of mean EJP/mEJP amplitudes, after correcting for nonlinear summation using a reversal potential of 0 mV (Chang et al., 1994). With 1 mM external $Ca^{2+}$, quantal content in homozygous $hsc4^{3550}$, homozygous $hsc4^{\Delta 19}$, and the trans-heterozygous combination of $hsc4^{\Delta 19}$ with the null alleles $hsc4^{\Delta 356}$ and $hsc4^{\Delta 11}$ was reduced to 31%–48% of control, but that of homozygous $hsc4^{R12}$ revertants was normal (Figure 4A). Because the loss of evoked release in homozy-

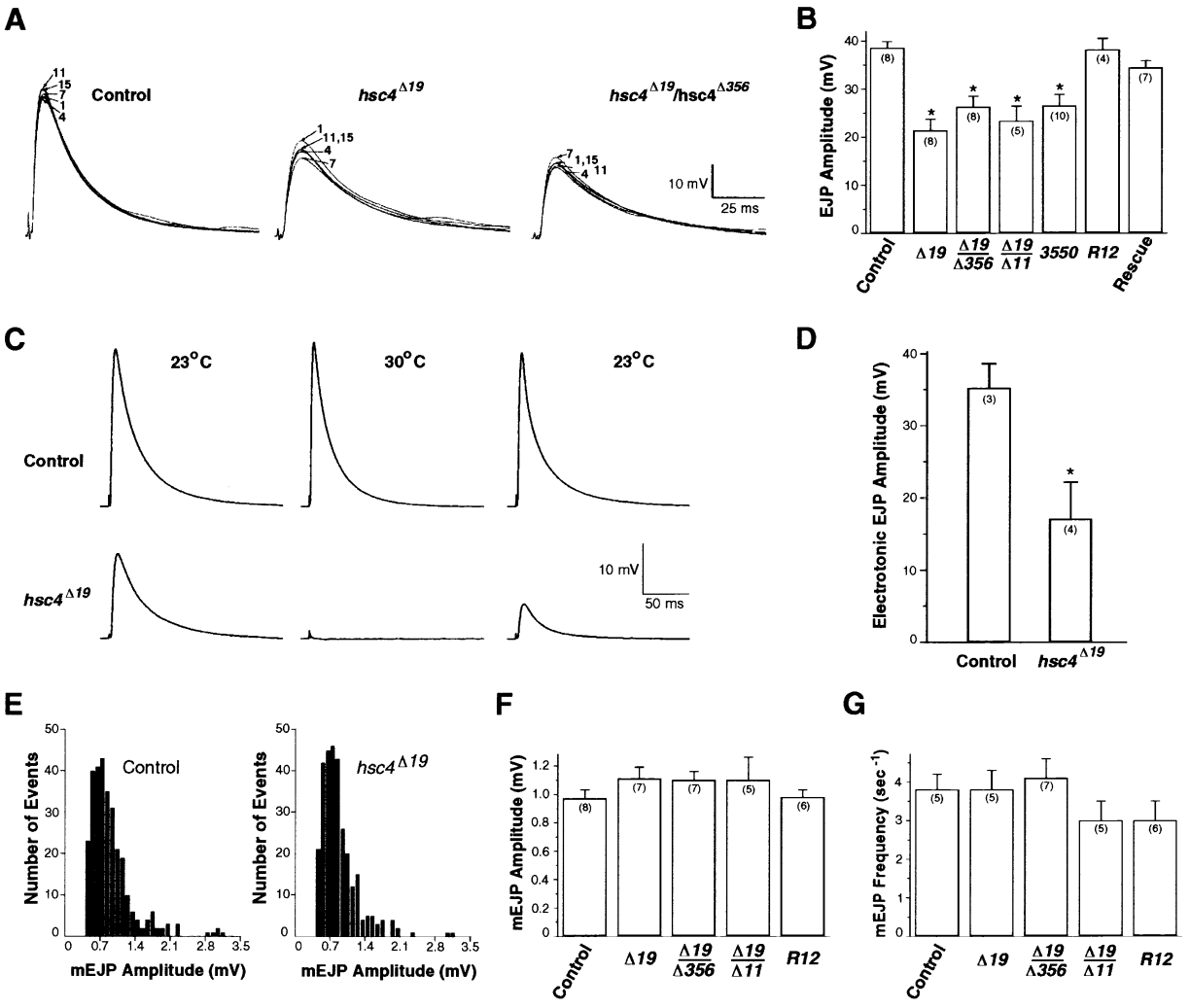


Figure 2. Nerve-Evoked Neurotransmitter Release Is Reduced at *hsc4* Mutant NMJs

(A–G) Nerve-evoked EJPs and spontaneous mEJPs were recorded from muscle 6 of control (wild-type Berlin) and mutant 3rd instar larvae. EJPs were elicited at 0.2 Hz with 1 mM $[Ca^{2+}]_e$. Fifteen responses obtained from each larvae were averaged. Control and *hsc4* mutant muscles exhibited similar resting potentials and membrane resistances (data not shown). Numbers in parentheses represent number of larvae recorded.

(A) Representative single EJP traces recorded at 23°C from control, homozygous $hsc4^{\Delta 19}$, and trans-heterozygous $hsc4^{\Delta 19/\Delta 356}$ mutant larvae. Each set of traces represents the 1st, 4th, 7th, 11th, and 15th response.

(B) Mean nerve-evoked EJP amplitudes at 23°C. The control EJP amplitude (39 ± 1 mV) was significantly different from that of homozygous $hsc4^{\Delta 19}$ mutants (21 ± 2 mV), $hsc4^{\Delta 19/\Delta 356}$ mutants (26 ± 2 mV), $hsc4^{\Delta 19/\Delta 11}$ mutants (23 ± 3 mV), and homozygous $hsc4^{3550}$ mutants (27 ± 2 mV). EJP amplitudes from homozygous $hsc4^{R12}$ revertants (38 ± 2 mV) and *P[hsc4]/+; hsc4*$^{\Delta 19/\Delta 19}$ larvae (34 ± 1 mV; "rescue") were similar to controls.

(C) Temperature dependence of evoked neurotransmitter release. Each row represents typical mean of 15 EJP traces recorded from the same larval NMJ of control and homozygous $hsc4^{\Delta 19}$ larvae at the indicated temperatures. $hsc4^{\Delta 19}$ mutants showed a loss of evoked release after 20–60 min at 30°C. Six out of eight mutant larvae showed no response at 30°C after 20 min, and showed an immediate partial recovery after cooling the preparation to 23°C.

(D) Electrotonically elicited EJP amplitudes. The mean EJP amplitude from control (35 ± 3 mV) was significantly different from that of homozygous $hsc4^{\Delta 19}$ larvae (17 ± 5 mV).

(E) Cumulative mEJP amplitude distribution for control and homozygous $hsc4^{\Delta 19}$. Each represents 300 events.

(F) Mean mEJP amplitudes. Control mEJP amplitudes (1.0 ± 0.1 mV) were similar to those of homozygous $hsc4^{\Delta 19}$ mutants (1.1 ± 0.1 mV), $hsc4^{\Delta 19/\Delta 356}$ mutants (1.0 ± 0.1 mV), $hsc4^{\Delta 19/\Delta 11}$ mutants (1.1 ± 0.2 mV), or homozygous $hsc4^{R12}$ revertants (1.0 ± 0.1 mV).

(G) Mean mEJP frequencies. Control mEJP frequencies (3.8 ± 0.4 $s^{-1}$) were similar to those of homozygous $hsc4^{\Delta 19}$ mutants (3.8 ± 0.5 $s^{-1}$), $hsc4^{\Delta 19/\Delta 356}$ mutants (4.1 ± 0.5 $s^{-1}$), $hsc4^{\Delta 19/\Delta 11}$ mutants (3.0 ± 0.5 $s^{-1}$), or homozygous $hsc4^{R12}$ revertants (3.0 ± 0.5 $s^{-1}$).

gous $hsc4^{\Delta 19}$ was not different from that of trans-heterozygous $hsc4^{\Delta 19}$ combinations with the null alleles $hsc4^{\Delta 356}$ and $hsc4^{\Delta 11}$, $hsc4^{\Delta 19}$ is at least a strong hypomorphic mutation at the larval NMJ.

We further examined the $Ca^{2+}$ dependence of quantal content at various low external $Ca^{2+}$ concentrations ($[Ca^{2+}]_e$) to estimate the $Ca^{2+}$ sensitivity and $Ca^{2+}$ cooperativity of evoked release (Dodge and Rahamimoff, 1967; Jan and Jan, 1976). For all $[Ca^{2+}]_e$s examined, the $[Ca^{2+}]_e$-quantal content relationship in $hsc4^{\Delta 19}$ mutants

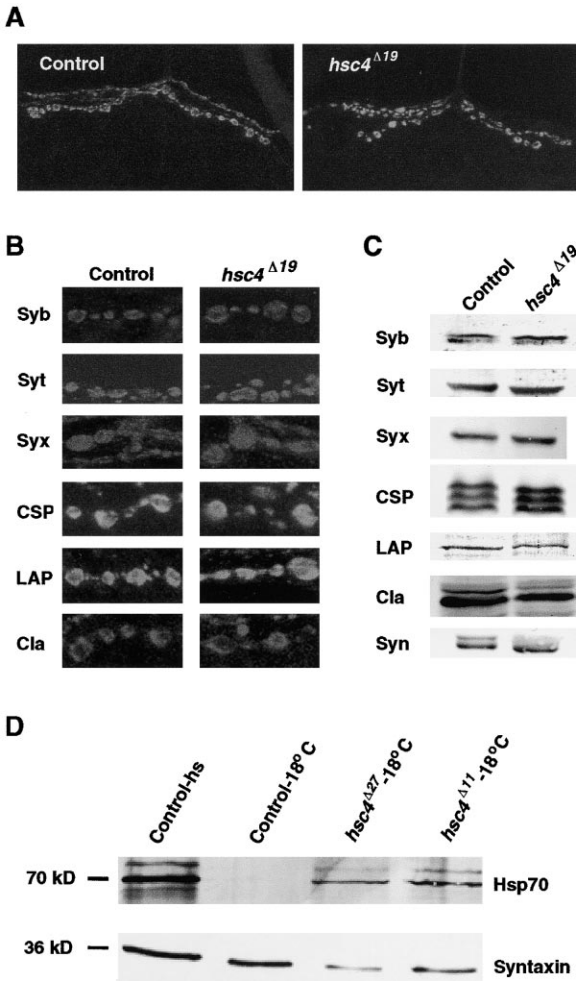


Figure 3. Distribution of Synaptic Proteins at *hsc4* Mutant NMJs

(A) Confocal image of larval NMJs (muscle 12) immunostained with anti-CSP antibodies in control and homozygous $hsc4^{\Delta 19}$ mutants. The morphological appearance of mutant NMJs was within the variation of control NMJs.

(B) Typical confocal images of synaptic boutons of NMJs 6/7 in control and homozygous $hsc4^{\Delta 19}$ larvae. NMJs were stained with antibodies against synaptobrevin I (Syb), synaptotagmin (Syt), syntaxin (Syx), CSP, LAP (AP180 homologue), and clathrin (Cla). No difference in mean fluorescence intensities of any staining was observed between control and mutants.

(C) SDS-PAGE separated protein extracts from control and homozygous $hsc4^{\Delta 19}$ 3rd instar larval brains were immunostained with antibodies against Syb, Syt, Syx, CSP, LAP, Cla, and synapsin (Syn). No consistent difference in protein expression was observed in at least four independent experiments.

(D) Protein extracts were obtained from 1st instar larvae of control, homozygous $hsc4^{\Delta 27}$ and $hsc4^{\Delta 11}$ mutants raised at 18°C, separated by SDS-PAGE, and immunostained with antibodies against Hsp70 and syntaxin (loading control). Positive control larvae for Hsp70 expression were heat-shocked for 2 hr at 37°C.

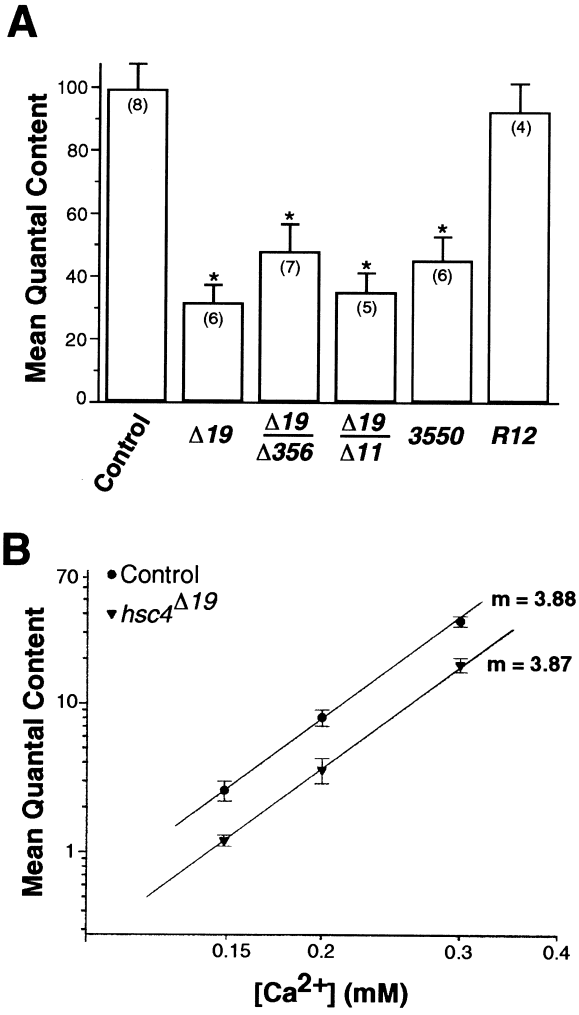


Figure 4. $Ca^{2+}$ Sensitivity but not $Ca^{2+}$ Cooperativity of Multiquantal Neurotransmitter Release Is Reduced at *hsc4* Mutant NMJs

(A) Quantal content at 1 mM $[Ca^{2+}]_e$. The mean estimated quantal content from larval muscle 6 of control (99 ± 8) was significantly different from homozygous $hsc4^{\Delta 19}$ mutants (32 ± 6), $hsc4^{\Delta 19/\Delta 356}$ mutants (48 ± 9), $hsc4^{\Delta 19/\Delta 11}$mutants (35 ± 6), and homozygous $hsc4^{P1594}$ mutants (45 ± 7), but not from that of $hsc4^{R12}$ revertants (92 ± 9).

(B) $[Ca^{2+}]_e$-quantal content relationship. Estimated quantal content in homozygous $hsc4^{\Delta 19}$ mutants was significantly reduced for each examined $[Ca^{2+}]_e$. Each point represents mean from 15 responses at 0.2 Hz from three larvae for 0.15 mM $Ca^{2+}$ and seven larvae for 0.2 and 0.3 mM $Ca^{2+}$. Lines were fitted by regression to each plot for control and $hsc4^{\Delta 19}$ larvae (m, slope).

was considerably shifted, such that higher levels of external $Ca^{2+}$ were required to evoke a given level of quantal release (Figure 4B). However, the slope of the relationship was normal in $hsc4^{\Delta 19}$ mutants. Together, these results indicate that the loss of Hsc4 does not affect the number of cooperative $Ca^{2+}$ binding sites needed to release a given quanta, but changes other $Ca^{2+}$-sensitive properties of neurotransmitter release.

### A Defect in Exocytosis Downstream of $Ca^{2+}$ Entry Causes the Loss of Neurotransmission in $hsc4^{\Delta 19}$ Mutants

To test whether the loss of nerve-evoked neurotransmitter release might be due to a loss of depolarization-dependent $Ca^{2+}$ entry, we used the $Ca^{2+}$ indicator Fluo-4 AM to measure relative levels of $[Ca^{2+}]_i$ in presynaptic

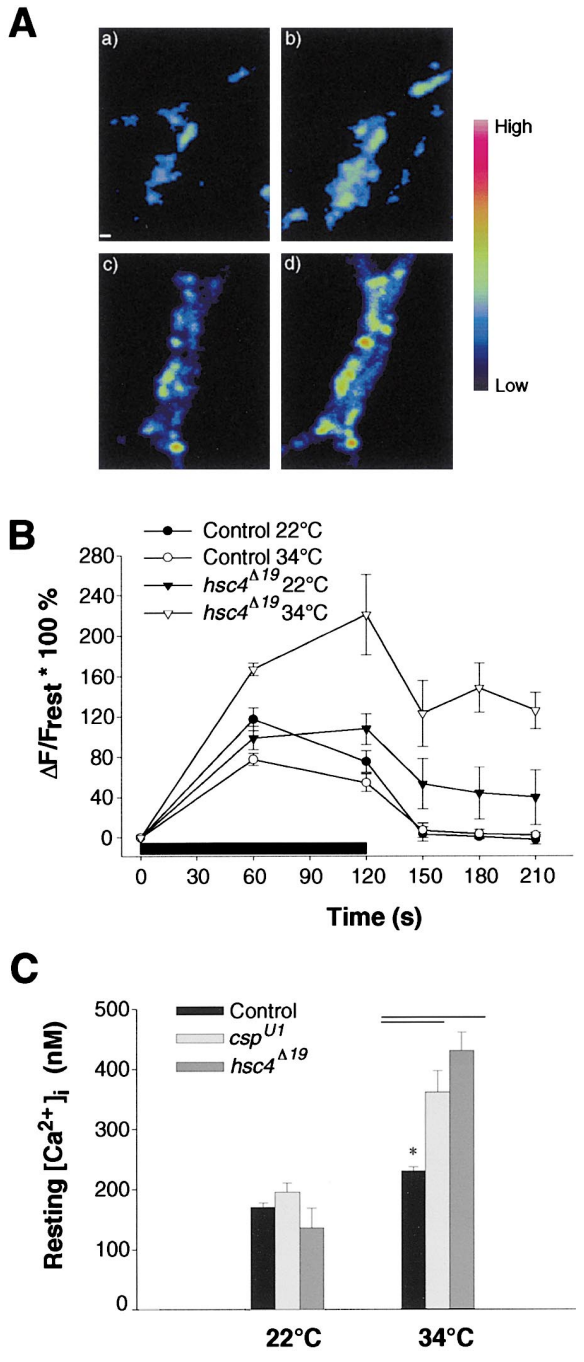


Figure 5. Mutations in Hsc4 Impair Neurotransmitter Exocytosis Downstream of $Ca^{2+}$ Entry

(A) Representative images showing boutons of NMJs 6/7 loaded with the $Ca^{2+}$ indicator Fluo-4 AM at 34°C before stimulation in control (a) and homozygous *hsc4*$^{\Delta 19}$ mutants (c). After stimulating at 10 Hz for 2 min *hsc4*$^{\Delta 19}$ mutant boutons (d) showed a much larger fluorescence change than controls (b). Scale bar represents 5 μm. (B) Relative changes in intraterminal $Ca^{2+}$ in type Ib boutons of both control and *hsc4*$^{\Delta 19}$ mutants at 22°C and 34°C, during and after 120 s of stimulation at 10 Hz (horizontal bar). Significant differences were observed between all curves (ANOVA) except for controls at 22°C and 34°C. During stimulation at 22°C, the $Ca^{2+}$ signal for both controls and *hsc4*$^{\Delta 19}$ plateaued with a relative change of approximately 90%. The longer decay of the $Ca^{2+}$ signal at 22°C in *hsc4*$^{\Delta 19}$ (43% ± 23%) compared to control (0.2% ± 4%) caused a statistical difference between these two groups (Student Newman-Keuls). At 34°C, there was a significant 4-fold larger signal in *hsc4*$^{\Delta 19}$ (221% ± 40%) than in controls (54% ± 9%). The decay of the Fluo-4 signal in *hsc4*$^{\Delta 19}$ was much slower at 34°C (136% ± 20%) than at 22°C. (C) Estimated $[Ca^{2+}]_i$ at rest for *Drosophila* type Ib boutons using Fura-2 AM are shown for control, *hsc4*$^{\Delta 19}$, and *csp*$^{U1}$ boutons (taken from Dawson-Scully et al., 2000). No difference was found between any groups at 22°C. However, at 34°C $[Ca^{2+}]_i$ at rest was significantly higher in both *hsc4*$^{\Delta 19}$ and *csp*$^{U1}$ mutant boutons compared with controls. No significant differences were observed between *csp*$^{U1}$ and *hsc4*$^{\Delta 19}$.

terminals of control and homozygous *hsc4*$^{\Delta 19}$ before, during, and after nerve stimulation at 10 Hz for 120 s (Figures 5A and 5B). Typically, control $Ca^{2+}$ signals increased to a maximum value in 60 s at 22°C (117% ± 12%) and at 34°C (78% ± 6%). After stimulation, $Ca^{2+}$ signals rapidly declined to resting levels. At 22°C, $Ca^{2+}$ signals in homozygous *hsc4*$^{\Delta 19}$ terminals showed an initial increase similar to controls after 60 s, but moderately increased levels after 120 s. At 34°C, however, $Ca^{2+}$ signals in *hsc4*$^{\Delta 19}$ were much increased at all examined time points during stimulation. The decay ($Ca^{2+}$ clearance) of Fluo-4 signals was slower in *hsc4*$^{\Delta 19}$ than in controls at both temperatures, although much more pronounced at 34°C (Figure 5B).

The similar (at 22°C) or increased levels (at 34°C) of nerve-evoked Fluo-4 fluorescence in *hsc4*$^{\Delta 19}$ terminals could suggest that a primary defect of $Ca^{2+}$ triggered exocytosis may be partially compensated by increased $Ca^{2+}$ entry. Alternatively, the level of $[Ca^{2+}]_i$ at rest could be actually lower in *hsc4*$^{\Delta 19}$ than in control. If so, the observed relative changes in Fluo-4 fluorescence would not necessarily indicate a larger $Ca^{2+}$ accumulation, because peak fluorescence values were normalized to resting values. We addressed this problem by measuring resting values of $[Ca^{2+}]_i$ using the ratiometric $Ca^{2+}$ indicator Fura-2 AM (Figure 5C). At 22°C, no significant difference in resting $[Ca^{2+}]_i$ was apparent between control (173 ± 7 nM) and *hsc4*$^{\Delta 19}$ mutant terminals (136 ± 33 nM). However, at 34°C, *hsc4*$^{\Delta 19}$ terminals exhibited significantly higher resting levels of $[Ca^{2+}]_i$ (430 ± 31 nM) than control (233 ± 8 nM), indicating a defect in $Ca^{2+}$ clearance at 34°C.

Our results suggest that nerve-evoked cytosolic $Ca^{2+}$ levels during stimulation attain similar or higher values in *hsc4*$^{\Delta 19}$ mutants than in control boutons. This was indicated by normal resting levels of $[Ca^{2+}]_i$ at 22°C and normal nerve-evoked Fluo-4 signals in *hsc4*$^{\Delta 19}$ terminals. At 34°C, evoked $Ca^{2+}$ entry was also not reduced in mutant boutons, because resting levels of $[Ca^{2+}]_i$ and evoked Fluo-4 signals were increased. Thus, it is unlikely that the loss of neurotransmitter release in *hsc4* mutants is primarily caused by a defect of $Ca^{2+}$ entry. Instead, these results point toward a defect in exocytosis downstream of $Ca^{2+}$ entry, which could be due to defects in synaptic vesicle recycling, the size of the readily releasable vesicle pool, the pathway triggering $Ca^{2+}$-dependent fusion, or vesicle fusion.

### Synaptic Vesicle Recycling at *hsc4*$^{\Delta 19}$ NMJs Is Normal

Because Hsc70 uncoats clathrin-coated vesicles in vitro and in vivo (Rothman and Schmid, 1986; Newmyer and

Schmid, 2001), an accumulation of clathrin-coated vesicles and a depletion of clear synaptic vesicles were likely to reduce exocytosis in *hsc4*$^{\Delta 19}$ terminals. However, ultrastructural studies of 3rd instar larval NMJs showed that homozygous *hsc4*$^{\Delta 19}$ mutant terminals contain a large number of clear synaptic vesicles similar to control (Figure 6A). As in control boutons, clathrin-coated vesicles in homozygous *hsc4*$^{\Delta 19}$ mutant boutons were also not detectable, suggesting that *hsc4*$^{\Delta 19}$ does not significantly interfere with the uncoating of clathrin-coated vesicles at larval NMJs.

To strengthen the ultrastructural studies, we investigated the physiology of synaptic vesicle recycling with two different assays. We measured activity-dependent membrane uptake with the fluorescent styryl dye FM1-43 (Betz and Bewick, 1992), because a block in clathrin-uncoating should accumulate freshly endocytosed vesicles. Concurrently, impaired recycling should also lead to an abnormal fatigue of neurotransmitter release during prolonged high frequency stimulation. To combine both assays, we recorded nerve-evoked EJPs in the presence of FM1-43 dye during 5 min of stimulation at 10 Hz and subsequently measured the intensity of FM1-43 uptake. For these experiments, we used 2 mM $[Ca^{2+}]_e$ to counteract the exocytotic defect in *hsc4*$^{\Delta 19}$ (see Figure 7D). Consistent with the ultrastructural studies, neither the amount of FM1-43 dye uptake (Figure 6B) nor the ability to sustain normal release during 10 Hz stimulation (Figure 6C) were substantially affected in homozygous *hsc4*$^{\Delta 19}$ terminals. Stimulation at 30 Hz for a period of 10 min also did not cause a notable difference in FM1-43 signals or EJP rundown between *hsc4*$^{\Delta 19}$ and control (data not shown). Together, these results suggest that vesicle recycling is normal at larval NMJs of *hsc4*$^{\Delta 19}$, excluding the possibility that the observed loss of neuroexocytosis is due to a reduced number of recycled vesicles.

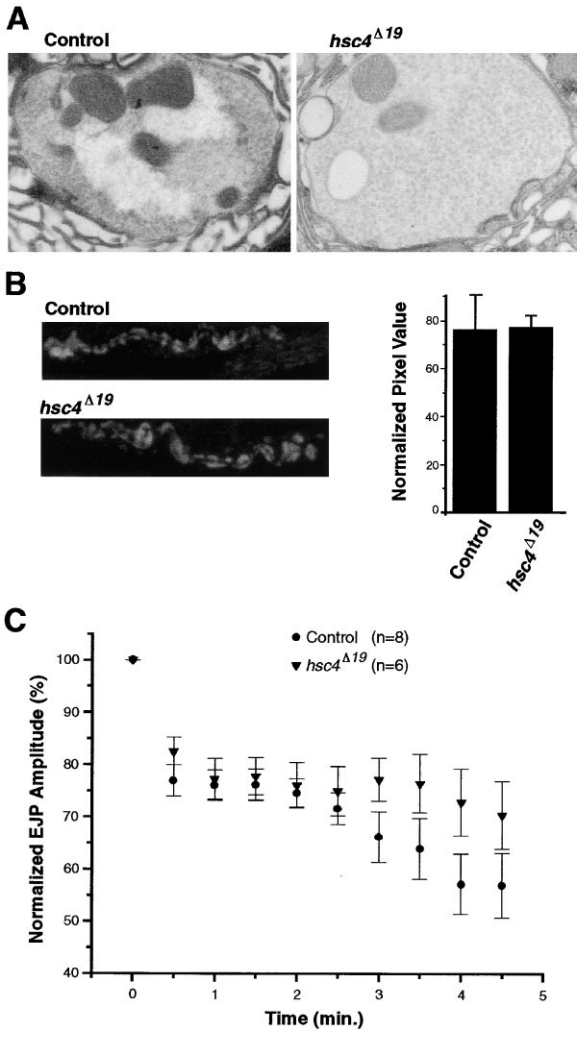


Figure 6. Synaptic Vesicle Recycling Is Normal in *hsc4* Mutants

(A) Electron micrographs of synaptic boutons from NMJs from muscles 6/7. As in controls, homozygous *hsc4*$^{\Delta 19}$ boutons contained a large complement of synaptic vesicles and showed no clathrin-coated vesicles (n = 10). Magnification 30,000×.

(B) Activity-dependent FM1-43 dye uptake. Motor neurons innervating muscle 6/7 of 3rd instar larvae were stimulated at 10 Hz for 5 min in the presence of FM1-43 dye and 2 mM $[Ca^{2+}]_e$. After washing in $Ca^{2+}$-free saline for 40 min at 4°C, the intensity of FM1-43 dye uptake was determined by subtracting muscle background from the mean pixel intensities of each examined bouton (3 μm). Left panel: Representative confocal images of FM1-43 dye uptake after stimulation. Right panel: Quantification of FM1-43 fluorescence revealed no difference in FM1-43 uptake between homozygous *hsc4*$^{\Delta 19}$ mutants (78 ± 2) and control (77 ± 10). N = 4 larvae for each genotype.

(C) Normalized mean EJP amplitudes obtained from experiments shown in (B). Mean amplitudes of 10 EJPs for each time point were normalized to the mean EJP amplitude of the first three responses. Mutant and control EJP amplitudes were statistically similar for each time point.

### A Step in the $Ca^{2+}$-Signaling Pathway Triggering Exocytosis Is Impaired in *hsc4*$^{\Delta 19}$ Mutants

Having established that the *hsc4*$^{\Delta 19}$ mutation affects a step of exocytosis, we tested the possibility that a reduced number of releasable vesicles might limit exocytosis. Because this population of vesicles can be measured by the depression of evoked release during repetitive stimulation (Liu and Tsien, 1995; Takahashi et al., 2000), we recorded excitatory junctional currents (EJCs) during a train of ten stimulation pulses elicited at 30 Hz. At a $[Ca^{2+}]_e$ of 1 mM, control EJC responses at the end of the train were depressed to 77% ± 3% of the initial response (Figure 7A). However, EJC responses recorded from homozygous *hsc4*$^{\Delta 19}$ mutants did not depress at all; instead, they were facilitated to 177% ± 14% of their initial value. Consequently, the striking facilitation of release in *hsc4*$^{\Delta 19}$ is inconsistent with the hypothesis that a reduced pool size of readily releasable vesicles might limit exocytosis.

Because facilitation of release during repetitive stimulation is apparently caused by an accumulation of residual $Ca^{2+}$ (Capogna, 1998; Zucker, 1989), it is likely that residual $Ca^{2+}$ counteracted any defects reducing exocytosis in *hsc4*$^{\Delta 19}$. Consistently, the facilitation of release in *hsc4*$^{\Delta 19}$ could be reverted by increasing the release probability with a higher $[Ca^{2+}]_e$. At 4 mM, 30 Hz stimulation depressed release in control and *hsc4*$^{\Delta 19}$ (Figure 7B), suggesting that the amount of release in *hsc4*$^{\Delta 19}$ reached a level similar to control, which became limited by the size of readily releasable pool or presynaptic $Ca^{2+}$ current inactivation. Examination of absolute EJC

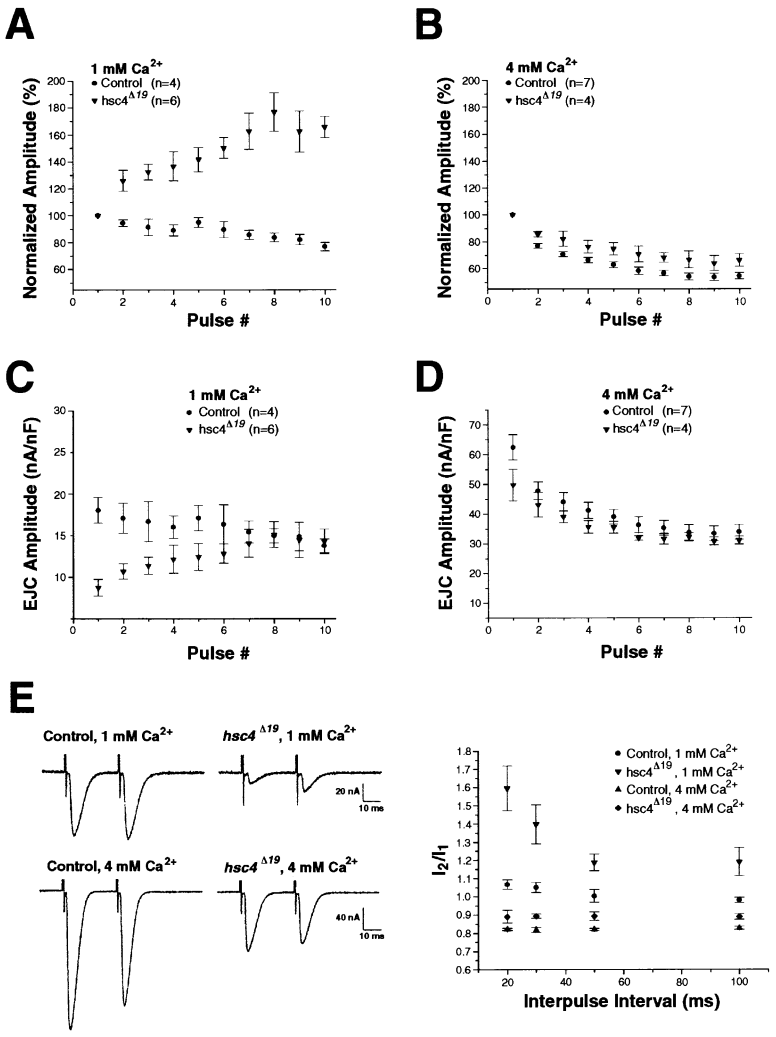


Figure 7. Repetitive Stimulation or High External $Ca^{2+}$ Counteracts the Loss of Neurotransmitter Release in *hsc4* Mutants

(A–D) Recordings of 10 EJCs elicited at 30 Hz while muscle 6 was clamped at −80 mV by a two-electrode voltage clamp at 23°C.

(A) With 1 mM $[Ca^{2+}]_e$, normalized control responses were depressed to 77% ± 3% of the initial response while *hsc4*$^{\Delta 19}$ mutant responses were facilitated to 177% ± 14%. Points represent the mean EJC response for a given stimulus pulse of n larvae normalized to the first response. For stimuli 2 through 10, the normalized responses were significantly different.

(B) With 4 mM $[Ca^{2+}]_e$, normalized control responses were depressed to 54% ± 3% and *hsc4*$^{\Delta 19}$ mutant responses were depressed to 64% ± 6%. The second mutant response was significantly different from the second response of control, but responses 3 through 10 were not.

(C) Absolute mean EJC amplitudes from (A), corrected for muscle size by dividing the EJC amplitude by the muscle cell capacitance. Control and homozygous *hsc4*$^{\Delta 19}$ mutant amplitudes were significantly different up to the third response.

(D) Absolute mean EJC amplitudes from (B). There was no significant difference between all control and *hsc4*$^{\Delta 19}$ mutant responses including the first response.

(E) Recordings of EJCs elicited by paired-pulse stimulation. Traces show typical averaged responses (n = 20) at a 30 ms interpulse interval from control and homozygous *hsc4*$^{\Delta 19}$. Mean EJC ratios (I2/I1) are shown from 20 consecutive paired stimuli (separated by 5 s) at 20–100 ms interpulse intervals. At 1 mM $[Ca^{2+}]_e$, *hsc4*$^{\Delta 19}$ mutant current ratios were significantly increased compared to control at all interpulse intervals except for 100 ms. At 4 mM $[Ca^{2+}]_e$, control and *hsc4*$^{\Delta 19}$ mutant ratios were similar.

amplitudes evoked by the 30 Hz train confirmed this idea (Figures 7C and 7D). At 1 mM $[Ca^{2+}]_e$, the first two EJC amplitudes recorded from *hsc4*$^{\Delta 19}$ were significantly different from control, while subsequent amplitudes were statistically similar. At 4 mM $[Ca^{2+}]_e$, evoked release was normal in *hsc4*$^{\Delta 19}$, because the absolute amplitude of the first EJC was already not significantly different from control. Together, these results indicate that increasing amounts of external and internal (residual) $Ca^{2+}$ counteract an apparently reduced probability of vesicle fusion in *hsc4*$^{\Delta 19}$.

Finally, we tested whether the abnormal facilitation in *hsc4*$^{\Delta 19}$ depends on the stimulation frequency by using paired stimulation pulses, which were 20 to 100 ms apart (Figure 7E). At a $[Ca^{2+}]_e$ of 1 mM, control responses maintained a paired-pulse ratio ($I_2/I_1$) close to 1 for all interpulse intervals indicating little or no facilitation. In contrast, *hsc4*$^{\Delta 19}$ responses exhibited a ratio of 1.6 ± 0.1 for a 20 ms interval; longer intervals progressively reduced the ratio to 1.2 ± 0.1. For a 100 ms interval, the mutant ratio was no longer statistically different from control, demonstrating that the facilitation in *hsc4*$^{\Delta 19}$ is frequency dependent, consistent with an accumulation of residual $Ca^{2+}$ counteracting the deficit of *hsc4* mutant synapses. Consequently, we conclude that the loss of exocytosis in *hsc4* mutant synapses is caused by an abnormally low probability of vesicle fusion due to a decreased sensitivity of the $Ca^{2+}$-signaling pathway triggering fusion.

### Hsc4 and CSP Act in the Same Signaling Pathway of Neurotransmitter Exocytosis

The defects in neurotransmitter release of *hsc4*$^{\Delta 19}$ mutants were surprisingly similar to those of *csp* null mutants (Umbach and Gundersen, 1997; Umbach et al., 1994; Dawson-Scully et al., 2000), suggesting that CSP and Hsc4 might act in the same signaling pathway. To further test this possibility, we confirmed that both proteins interact in vitro. Using an anti-CSP antibody affinity column, Hsc4 was coimmunopurified with CSP in an ATP-dependent manner (Figure 8A). Controls did not copurify Hsc4 (Figure 8B), suggesting that the copurification of Hsc4 with CSP is specific. The small amount of coisolated CSP-Hsc4 complexes (Figure 8B) was comparable to studies with mammalian proteins (Braun et al., 1996; Chamberlain and Burgoyne, 1997), sug-

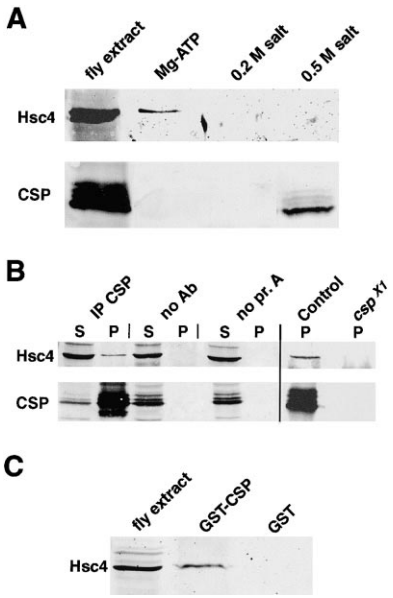


Figure 8. Hsc4 Interacts with CSP In Vitro

(A) Copurification of Hsc4 with CSP from fly head extracts using an anti-CSP antibody affinity column. Bound proteins were sequentially eluted with $Mg^{2+}$-ATP, 0.2 M imidazole, and 0.5 M imidazole. Pooled protein fractions were separated by SDS-PAGE and immunostained for Hsc4 and CSP. Note the appearance of a 70 kDa immunopositive signal for Hsc4 in the $Mg^{2+}$-ATP elution and 32–36 kDa signals for CSPs in the high salt elution.

(B) Left panel: Immunoprecipitation of CSP (IP CSP) from head extracts of control flies. Controls either omitted CSP antibody (no Ab) or protein A coupled beads (no pr. A). The supernatant (S) and the precipitated fraction (P) were analyzed on separate blots for the presence of CSP and Hsc4. Controls showed neither a CSP nor a Hsc4 specific signal. Right panel: CSP antibodies copurified Hsc4 from extracts of control, but not of $csp^{X1}$ deletion mutants.

(C) A solubilized protein head extract (fly extract) was incubated with immobilized glutathione-S-transferase-CSP (GST-CSP) fusion protein or for a control, with an equal amount of immobilized GST. After washing, bound proteins were eluted with 50 mM glutathione.

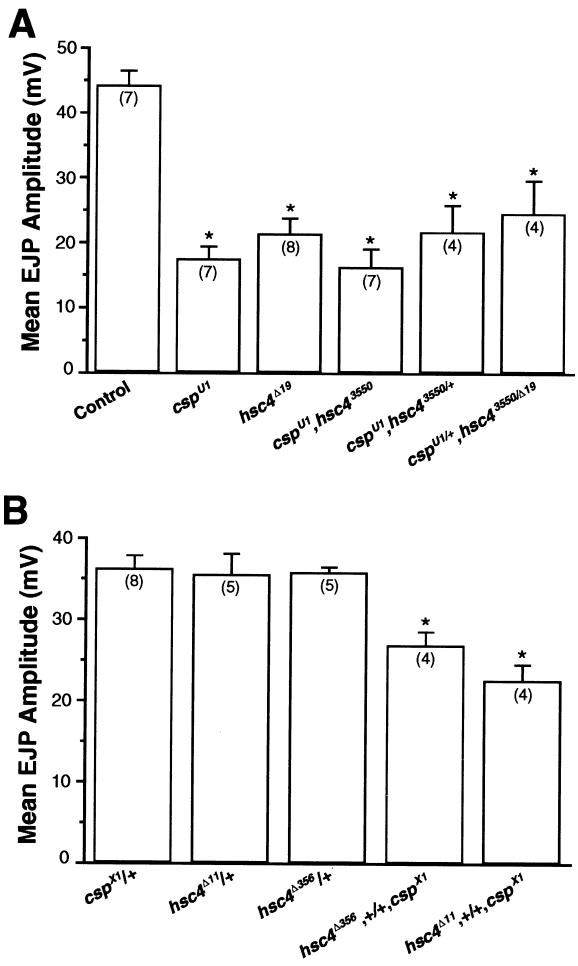


Figure 9. Hsc4 Interacts with CSP in Common Signaling Pathways

(A) Nerve-evoked release in homozygous *hsc4*, *csp*, and *hsc4-csp* double mutants. EJPs were recorded from muscle 6 at 23°C with 1 mM $[Ca^{2+}]_e$. Mean EJP amplitudes recorded from homozygous $csp^{U1}$, $hsc4^{3550}$ double mutant larvae (16 ± 3 mV) were significantly reduced when compared to control (44 ± 2 mV). Mean EJPs from either homozygous $hsc4^{\Delta 19}$ (21 ± 2 mV) or $csp^{U1}$ (17 ± 2 mV) NMJs were similar to that of double mutants. EJPs from control combinations $csp^{U1/U1}$, $hsc4^{3550/+}$ (22 ± 4 mV) and $csp^{U1/+}$, $hsc4^{3550/\Delta 19}$ (25 ± 5 mV) were similar to $csp^{U1}$, $hsc4^{3550}$ double mutants. Number of recorded larvae is indicated in parentheses.

(B) Nerve-evoked release in heterozygous *hsc4*, *csp*, and *hsc4-csp* double mutants. Recordings as in (A). Mean EJPs recorded from transheterozygous $hsc4^{\Delta 356/+}$,$csp^{X1/+}$ (27 ± 2 mV) and transheterozygous $hsc4^{\Delta 11/+}$,$csp^{X1/+}$ double mutant larvae (23 ± 2 mV) were significantly reduced when compared to heterozygous $csp^{X1/+}$ (36 ± 2 mV), heterozygous $hsc4^{\Delta 356/+}$ (36 ± 2 mV), or heterozygous $hsc4^{\Delta 11/+}$ larvae (36 ± 1 mV).

gesting that the interaction between both proteins is unstable. Finally, Hsc4-CSP protein complexes could also be formed in vitro, as demonstrated by "pull-down assays" of native Hsc4 with recombinant CSP fusion protein (Figure 8C). Together these in vitro studies suggest that Hsc4 interacts with CSP in an ATP-dependent manner consistent with results obtained in mammalian systems (Braun et al., 1996; Chamberlain and Burgoyne, 1997).

To gather compelling in vivo evidence for a Hsc4-CSP interaction, we used genetic recombination to generate double mutant flies, which are homozygous for $hsc4^{3550}$ and $csp^{U1}$, a null allele of CSP (Zinsmaier et al., 1994). If both proteins act in the same signaling pathway, one expects that double mutant flies exhibit the same phenotypical features as each individual mutation. Consistent with this idea, EJP amplitudes recorded from homozygous $hsc4^{3550}$-$csp^{U1}$ double mutant NMJs were reduced to 37% ± 6% of control amplitudes (Figure 9A) and were statistically similar to the reduced EJP amplitudes recorded from individual homozygous $hsc4^{3550}$ or $csp^{U1}$ mutant NMJs. The frequency and amplitudes of spontaneously occurring mEJPs in double mutants were not different from controls (data not shown). Furthermore, we examined trans-heterozygous *hsc4-csp* double mutant combinations of the *csp* null allele $csp^{X1}$ (Zinsmaier et al., 1994) with the stronger deletion alleles, $hsc4^{\Delta 356}$ and $hsc4^{\Delta 11}$, and found that nerve-evoked EJP amplitudes were significantly reduced in these synthetic mutants. EJP amplitudes in trans-heterozygous $hsc4^{\Delta 356/+}$-$csp^{X1/+}$ larvae were reduced to 75% ± 4% of control amplitudes, and to 63% ± 5% in $hsc4^{\Delta 11/+}$-$csp^{X1/+}$ larvae (Figure 9B). Together these

results suggest that both proteins are likely to form a complex that acts in the same signaling pathway leading to $Ca^{2+}$-triggered neurotransmitter exocytosis.

## Discussion

In this study, we genetically tested the function of the clathrin-uncoating ATPase Hsc70 at *Drosophila* motor nerve terminals. Of the five *hsc70* genes in *Drosophila*, we examined mutations in the *hsc4* gene, because this is considered the closest homolog to bovine Hsc70. The observed defects in *hsc4* mutant synaptic transmission suggest a primary role of Hsc4 in a direct step of exocytosis and a secondary role in protecting presynaptic $Ca^{2+}$ entry/clearance against thermal stress.

### Hsc4 Increases the Probability of $Ca^{2+}$-Triggered Synaptic Vesicle Fusion at Larval NMJs of *Drosophila*

The partial loss-of-function mutation $hsc4^{\Delta 19}$ significantly impairs synaptic transmission at larval NMJs by ~50%. The defect is clearly intrinsic to neurotransmitter release for two reasons. First, the normal amplitudes of unitary quantal release events indicated a normal postsynaptic physiology. Second, the loss of nerve-evoked release elicited in the presence or absence of action potentials was indistinguishable, indicating a defect downstream of nerve excitation. Together, these experiments localize the *hsc4* mutant defect to the presynaptic terminal.

To define the impaired mechanism of neurotransmitter release, we systematically examined presynaptic $Ca^{2+}$ levels at rest, evoked $Ca^{2+}$ levels, vesicle recycling, limitations of the readily releasable pool, the probability of release, and vesicle fusion. Fluo-4 AM imaging of stimulus-evoked $Ca^{2+}$ levels in presynaptic boutons of $hsc4^{\Delta 19}$ mutant NMJs revealed signals slightly above control at 22°C and significantly larger signals at 34°C. Because Fura-2 AM-measured $Ca^{2+}$ levels at rest were normal at 22°C, we conclude that the loss of evoked release at 22°C is not due to a lack of $Ca^{2+}$ entry, but more likely caused by an impaired step of exocytosis downstream of $Ca^{2+}$ entry. An additional role of Hsc4 in clearing $Ca^{2+}$ from nerve terminals at high temperatures was indicated by larger stimulus-evoked $Ca^{2+}$ signals at 34°C, their slow recovery to resting levels, and increased $Ca^{2+}$ resting levels at 34°C.

Although Hsc70 has been shown to uncoat clathrin-coated vesicles in vitro, the loss of synaptic transmission in the examined mutation $hsc4^{\Delta 19}$ could not be attributed to a defect in vesicle recycling for several reasons. First, the reduction of nerve-evoked release at low stimulation frequencies was not caused by a progressive run down of responses. Second, activity-dependent FM1-43 uptake was normal. Third, evoked responses showed normal depression kinetics during prolonged high frequency stimulation at a high $[Ca^{2+}]_e$. Fourth, no gross depletion of the total vesicle pool was evident in mutant terminals. Fifth, as in control, clathrin-coated vesicles were not detected in presynaptic terminals. Despite this apparent lack of a vesicle recycling defect in $hsc4^{\Delta 19}$ mutant NMJs, our results do not exclude a function of Hsc70 in clathrin-mediated endocytosis. Although a significant expression of Hsc4 was not detectable at $hsc4^{\Delta 19}$ NMJs, residual levels could still be sufficient for the clathrin-uncoating reaction. In addition, related Hsc70 isoforms could substitute for the loss of Hsc4 function. In particular, stress-induced Hsp70 expression was abnormally induced in *hsc4* mutants, although it remains unclear whether Hsp70 can bind clathrin.

A potential defect in the machinery refilling the readily releasable pool can also be excluded as a primary cause for the loss of release in *hsc4* mutants, because repetitive stimulation caused a striking facilitation of evoked release at a $[Ca^{2+}]_e$ at which control responses were depressed. If the size of the readily releasable pool limited release in the mutants, then depression rather than facilitation of release would have been expected. Furthermore, a defect in the machinery mediating or regulating the fusion pore is also not likely, because the frequency of spontaneously occurring release events were normal, and the rise and decay time constants of stimulus-evoked current responses were not decreased (data not shown).

The systematic exclusion of significant defects in $Ca^{2+}$ entry, vesicle recycling, the readily releasable pool, or vesicle fusion, leaves only one mechanism: the $Ca^{2+}$ signaling pathway triggering $Ca^{2+}$-dependent fusion. Because a failure of $Ca^{2+}$ entry is unlikely to cause the loss of release in *hsc4* mutants, the defect must be between the sensor and the fusion machinery. Although the molecular nature of the $Ca^{2+}$ sensor is not entirely understood, it is assumed from the fourth power relationship of neurotransmitter release with the $[Ca^{2+}]_e$ or $[Ca^{2+}]_i$ that four cooperative $Ca^{2+}$ binding sites are required to trigger fusion (Dodge and Rahamimoff, 1967; Bollmann et al., 2000; Schneggenburger and Neher, 2000). We examined this relationship in $hsc4^{\Delta 19}$ mutants, and found a normal $Ca^{2+}$ cooperativity but a reduced $Ca^{2+}$ sensitivity, indicating that the mutations do not interfere with $Ca^{2+}$ binding, but with a subsequent step of $Ca^{2+}$-triggered exocytosis.

Consistent with a reduced $Ca^{2+}$ sensitivity of vesicle fusion, $hsc4^{\Delta 19}$ mutants exhibited a striking facilitation of evoked release during repetitive stimulation at a $[Ca^{2+}]_e$ of 1 mM. Higher concentrations then lead to a depression of release. The degree of facilitation is inversely correlated with the probability of release such that any manipulation decreasing release probability, like reduced $[Ca^{2+}]_e$, results in an increase of facilitation (Capogna, 1998). Consistently, increasing the probability of release reverts facilitation and leads to depression (Capogna, 1998; Debanne et al., 1996), due to saturating $[Ca^{2+}]_i$, leading to an accelerated depletion of the readily releasable pool and presynaptic $Ca^{2+}$-current inactivation. Consequently, the facilitation of release in $hsc4^{\Delta 19}$ mutants at a $[Ca^{2+}]_e$ that depresses release in control, and the reversibility of facilitation with higher $[Ca^{2+}]_e$s, indicate that the probability of release is reduced. In addition, the fact that raising extracellular or intracellular $Ca^{2+}$ (through repetitive stimulation) counteracted the loss of release indicates that the $Ca^{2+}$ sensitivity of $Ca^{2+}$-triggered release must be decreased. Because the reduced $Ca^{2+}$ sensitivity was not caused by reduced $Ca^{2+}$ entry, nor by a change in the $Ca^{2+}$ cooperativity of release, we conclude that a defect of $Ca^{2+}$ signaling downstream of the $Ca^{2+}$ sensor and upstream of vesicle fusion

primarily impairs neurotransmitter release in *hsc4* mutants. This step is likely to adjust the probability of neurotransmitter release by regulating the $Ca^{2+}$ sensitivity of vesicle fusion.

### Hsc4 Cooperates with CSP to Mediate Neurotransmitter Exocytosis

A second focus of this study was to determine whether Hsc70 interacts with CSP in a common pathway mediating neurotransmitter release. Analyzing $hsc4^{\Delta 19}$ mutants, we found profound defects in evoked release, which are surprisingly similar to those observed in *csp* mutants. In particular, the *hsc4* mutant thermo-intolerant loss of evoked but not of spontaneous release, the reduced $Ca^{2+}$ sensitivity but normal $Ca^{2+}$ cooperativity of evoked release, the increased facilitation of release, the normal or increased levels of presynaptic $Ca^{2+}$ entry, the normal or increased presynaptic $Ca^{2+}$ resting levels, and the rescue of nerve-evoked release by high $[Ca^{2+}]_e$s or repetitive stimulation, are all hallmarks of the absence of CSP in *Drosophila* (Umbach et al., 1994; Umbach and Gundersen, 1997; Dawson-Scully et al., 2000).

The similar defects in synaptic transmission of loss-of-function mutations in CSP and Hsc4, suggest that both proteins may act in the same signaling pathway. This idea is further strengthened by the ATP-dependent in vitro interaction of Hsc4 and CSP. Furthermore, individual and homozygous double mutants of CSP and Hsc4 showed an indistinguishable loss of nerve-evoked release, suggesting that both proteins act in the same signaling pathway. Finally, trans-heterozygous double mutants of CSP and Hsc4 showed a significant reduction of evoked release, indicating a direct interaction. Together, these results suggest that Hsc4 and CSP are likely to form a vesicle-associated chaperone complex, which primarily increases the $Ca^{2+}$ sensitivity of $Ca^{2+}$-triggered vesicle fusion.

The suggested primary function of the CSP/Hsc70 complex is consistent with a series of studies using "slow" peptidergic secretion systems of mammals and *Drosophila*, which also indicate that CSP mediates a direct step of exocytosis (reviewed by Chamberlain and Burgoyne, 2000). In particular, a recent study in chromaffin cells showed that overexpression of CSP not only interferes with the amount of catecholamine release, but also with the kinetics of single release events, suggesting that CSP may act at a step close to the machinery facilitating or regulating the fusion pore (Graham and Burgoyne, 2000). The hypothesis that CSP, most likely in cooperation with Hsc70, may modulate sequential interactions of SNARE-associated proteins is supported by in vitro and in vivo interactions of CSP with syntaxin in *Drosophila* (Nie et al., 1999; Wu et al., 1999), and the copurification of synaptobrevin with CSP (Leveque et al., 1998).

The role of the CSP/Hsc70 complex at nerve terminals is apparently widespread and different from previous assumptions. CSP was originally suggested to promote the activity of presynaptic $Ca^{2+}$ channels (Gundersen and Umbach, 1992). However, this idea is not consistent with the observed defects in presynaptic $Ca^{2+}$ entry and clearance in motor terminals of *Drosophila* mutants. Specifically, *csp* mutants (Dawson-Scully et al., 2000), and to a lesser degree *hsc4* mutants, exhibit increased levels of stimulus-evoked intraterminal $Ca^{2+}$, indicating an inhibitory role on depolarization-dependent $Ca^{2+}$ entry. Such a role is consistent with the recent finding that coexpression of CSP promotes a G protein-mediated tonic inhibition of ectopically expressed N-type $Ca^{2+}$ channels (Magga et al., 2000). In addition, it is clear that the CSP/Hsc70 mediates a step of exocytosis and protects $Ca^{2+}$ clearance at nerve terminals against thermal stress.

### Conclusion

In this study, we provide evidence for two novel roles of Hsc70 at presynaptic nerve terminals. We show that loss of Hsc4 in *Drosophila* reduces stimulus-evoked neurotransmitter exocytosis at all temperatures and impairs presynaptic $Ca^{2+}$ clearance at elevated temperatures. We have also determined that Hsc4 and CSP interact in vitro and in a common in vivo signaling pathway. Our results support a model suggesting that vesicle-associated CSP recruits Hsc70 to synaptic vesicles to regulate or chaperone protein interactions mediating at least two functions at nerve terminals: increasing the $Ca^{2+}$ sensitivity of vesicle fusion and stabilizing $Ca^{2+}$ clearance against thermal stress. It will now be of interest to determine the protein interactions targeted by this chaperone system to facilitate exocytosis.

## Experimental Procedures

### Genetics and Molecular Analysis

The P element allele $hsc4^{3550}$ was obtained from the Bloomington Stock Center. A transgenic strain containing the rescue construct *P[hsc4]* (Hing et al., 1999) was kindly provided by S. Artavanis-Tsakonas (Massachusetts General Hospital Cancer Center, Charlestown, MA).

The P{PZ} element insertion site of $hsc4^{3550}$ was isolated by plasmid rescue and sequenced. Homozygous viable revertant and lethal deletion lines were generated by excision of the P element in $hsc4^{3550}$, essentially as previously described (Zinsmaier et al., 1994). Excisions were tested for complementation of $hsc4^{3550}$. Deletion breakpoints were initially identified by Southern blotting using genomic *hsc4* DNA and mapped in detail by sequencing PCR-amplified genomic DNA using the following primers: JW1 (GGCTGGGCAG CCG TGTGCG), JW2 (ACGCACGAGTAGGTGGTG CCC), JW5 (GTTA CCTTCCAAGTTGAATTGTGTG), JW13 (CAAACACACGCGCCCTCAC), JW16 (ACTGCATCCCCGCTGGTTGGG), and JW18 (TCACTGGCG TGTGTTTTGCGG). To determine the lethal stage and the synaptic physiology, *hsc4* mutant lines were balanced with *TM6*, *Tb* or *yw*; *TM3*, *Ser*, $y^+$. Wild-type Berlin (WTB) was used throughout this study as control, because $ry^{506}$ was physiologically indistinguishable from WTB.

### Immunohistochemistry

Embryo or larval antibody staining was performed with PBS containing 0.2% Triton-X 100 (PBT) after fixation with 2%–4% formaldehyde essentially as described (Zinsmaier et al., 1994). For clathrin antibody staining, larvae were fixed in Bouin's Fixative for 30 min at 22°C. Antibodies were diluted in PBT as follows: rabbit anti-Hsc4 at 1:100 (K. Palter, Temple University, Philadelphia, PA), mouse anti-CSP at 1:50 (ab49), goat anti-clathrin at 1:400 (Sigma, St. Louis, MO), mouse anti-Syntaxin at 1:50 (8C3, S. Benzer, California Institute of Technology, Pasadena, CA), rabbit anti-Synaptotagmin at 1:10,000 (DSYT-2, H. Bellen, Baylor College of Medicine, Houston, TX), anti-Synaptobrevin I at 1:15,000 (1769, R. Kelly, University of California San Francisco, San Francisco, CA), anti-LAP at 1:50 (G19, B. Zhang, University of Texas School of Biological Sciences, Austin, TX), anti-mouse FITC at 1:500, anti-goat Cy3 at 1:400, anti-rat FITC at 1:200, anti-mouse Cy3 at 1:300, and anti-rabbit Rhodamine at

1:200, anti-rabbit alkaline phosphatase at 1:200 (all from Jackson ImmunoResearch, West Grove, PA). Confocal images were taken using the same parameters for control and mutant larvae. Measurements of fluorescent staining intensities were made as described for FM1-43 imaging.

### Electrophysiology

Both voltage-clamp and current-clamp recordings were made from muscle 6 in the anterior ventral abdomen of climbing third instar larvae essentially as described previously (Dawson-Scully et al., 2000). Dissections were made in $Ca^{2+}$-free HL-3 solution (Stewart et al., 1994). The composition was (in mM): NaCl, 70; KCl, 5; $MgCl_2$, 20; $NaHCO_3$, 10; Trehalose, 5; HEPES, 5; Sucrose 115. For recordings, HL-3 solution was supplemented with $CaCl_2$ as indicated and continuously superfused over the preparation. To elicit a postsynaptic response, the segmental nerve was stimulated for 0.1 ms at two and a half to three times the stimulus amplitude required for a threshold response. Voltage signals were amplified with an Axopatch 1D amplifier (Axon Instruments, Foster City, CA), filtered at 1 kHz, and digitized at 5 kHz directly to disk with a DigiData 1200 interface and pClamp 6.0 software (Axon Instruments). Current signals were amplified with an Oocyte Clamp OC-725C (Warner Instrument Corp., Hamden, CT), filtered at 1 kHz, and digitized at 20 kHz directly to disk with a DigiData 1200 interface and pClamp 6.0 software. Evoked responses were analyzed with pClamp 6.0 software, spontaneous events with the Mini Analysis Program (Synaptosoft Inc., Leonia, NJ). Plots were made using Origin 4.0 (Microcal Software Inc., Northampton, MA).

### Calcium Imaging Procedures

Loading and $Ca^{2+}$ imaging of synaptic boutons with the calcium indicators Fluo-4 AM and Fura-2 AM was carried out essentially as described by Dawson-Scully et al. (2000), except for the erroneous final concentration values which appeared in this paper. Correct final concentrations are 100 nM TPEN (N,N,N′,N′-tetrakis (2-pyridylmethyl) ethlenediamine), 0.04% (wt/vol) pluronic acid, 1.4% (vol/vol) dimethyl sulfoxide and 0.0001% ethanol in Schneider's medium (Gibco BRL) for loading and in HL-3 solution for imaging. 12 μM Fluo-4 AM was used for loading, and 5 μM for imaging. Stimulus trains were delivered once. $Ca^{2+}$ signals were recorded from motor nerve terminals innervating muscle 6/7.

Images of 127 × 170 pixels were accumulated at 630 ms intervals. The fluorescence response, normalized to resting fluorescence ($\Delta F/F_{rest}$), was expressed as the change in fluorescence ($F_{stim} - F_{rest}$) divided by resting fluorescence ($F_{rest}$): $\Delta F/F_{rest}$ (%) = 100 × ($F_{stim} - F_{rest}$)/$F_{rest}$. Time constants of the $Ca^{2+}$ signal decay were obtained using nonlinear regression with a double variable exponential decay ($y = ae^{-bx} + ce^{-dx}$) fitted to the average signal following stimulation at each frequency.

### FM1-43 Assay

The FM1-43 uptake assay was essentially performed as described (Ranjan et al., 1998). FM1-43 dye uptake was stimulated with a suction electrode at 10 Hz in the presence of 8 μM FM1-43 dye and 2 mM $Ca^{2+}$ in HL-3. After washing in the dark for 30 min at 4°C in $Ca^{2+}$-free HL-3 solution containing 0.5 mM EGTA, FM1-43 staining was visualized with epifluorescent optics through fluorescein excitation (475 nm) and emission (520 nm) filters (Reichert Polyvar 2, Leica, Deerfield, IL). 12 bit images of stained NMJs were acquired using Open Lab software (Improvision, United Kingdom). The fluorescence intensity was measured from 8–12 stained boutons with diameters >3 nm. FM1-43 uptake was normalized by subtracting background muscle fluorescence. Mean values were determined from n larvae.

### Electron Microscopy

Third instar larvae were dissected as described previously. Larval tissues were fixed for 2 hr with 2.5% paraformaldehyde and 1.5% glutaraldehyde in HL-3 solution containing 1 mM $Ca^{2+}$ at room temperature, followed by an overnight fixation at 4°C in the same fixative. Poststaining and embedding was essentially as described (Zinsmaier et al., 1994). Transmission electron microscopy was performed from serial sections through boutons of muscle 6/7, and images were taken at 30,000× and 50,000× magnification.

### Immunopurification

Purified monoclonal anti-CSP antibody (ab49) was coupled to CNBr-activated Sepharose 4B beads (Pharmacia, Piscataway, NJ). Frozen fly heads were homogenized in buffer A (in mM: 50 KCl, 0.02 $CaCl_2$, 10 HEPES [pH 7.8]) using 0.5 ml heads/1 ml buffer. Crude extract was supplemented with protease inhibitors (0.1 mM PMSF, 100 ng/ml Pepstatin A, 3.3 μg/ml Aprotinin), solubilized with 3% Triton X-100 at 4°C for 2 hr, and cleared by a low-speed centrifugation for 10 min (2000 rpm, Sorval SS-35) and a high-speed centrifugation (27,000 rpm, Beckman SW28) for 60 min at 4°C. The supernatant was diluted with buffer A to 1% Triton X-100 and filtered (0.22 micron). After loading at 4°C, the column was washed with 10 vol of buffer B (in mM: 50 KCl, 0.02 $CaCl_2$, 10 Tris-HCl [pH 7.8], 1% Triton X-100) and 5 vol of 40 mM imidazole in buffer B. Proteins were eluted with 4 vol of 5 mM ATP, 2 mM $MgCl_2$ in buffer B, 4 vol 200 mM imidazole in buffer B, and 4 vol 500 mM imidazole in buffer B.

For small-scale immunoprecipitations, frozen fly heads were homogenized in buffer C (in mM: 50 KCl, 0.1 PMSF, 0.2% Triton X-100, 10 Hepes [pH 7.4]). The post-nuclear supernatant was incubated overnight with anti-CSP antibody at 4°C. IgGs were bound to Protein A-agarose beads (Pharmacia) for 2 hr, recovered by centrifugation, washed, and resuspended in SDS sample buffer.

### GST Pull-Down Assay

Recombinant GST-CSP fusion protein and GST protein were expressed in *E. coli* and immobilized to GST-agarose beads essentially as described (Zinsmaier et al., 1990). The amount of GST-CSP and GST bound to glutathione-agarose beads was estimated by Coomassie blue staining after SDS-PAGE using bovine serum albumin as the standard. Protein extract from 2.5 ml of fly heads was incubated at 4°C for 16 hr in buffer D (in mM: 50 KCl, 2 $MgCl_2$, 1 $CaCl_2$, 1 DTT, 10 HEPES [pH 7.4], 1% Triton X-100) with glutathione-agarose beads containing 80 μg of immobilized GST-CSP or GST protein. Bound proteins were recovered by centrifugation the pellet, washed, and extracted with GST-buffer (50 mM glutathione, 1% Triton X-100, 50 mM Tris-HCl [pH 8.0]). Eluted proteins were precipitated with TCA and resuspended in SDS-PAGE buffer.

### Immunoblotting

Protein fractions were fractionated by SDS-PAGE and analyzed by immunostaining using an alkaline phosphatase staining reaction as described (Zinsmaier et al., 1990). The following antibody dilutions were used: anti-CSP (ab49) at 1:100, anti-Hsc4 at 1:8000, anti-Hsp70 at 1:500 (7.10, Affinity Bioreagents, Neshanic Station, NJ), anti-syntaxin (8C3) at 1:50, anti-clathrin at 1:400, anti-synaptotagmin (DSYT-2) at 1:1000, anti-synaptobrevin at 1:2000, anti-LAP (G19) at 1:200, anti-synapsin at 1:50 (3C11, E. Buchner, University of Wuerzburg, Germany), anti-rabbit or anti-mouse antibody conjugated with alkaline phosphatase at 1:10,000.

### Statistical Analysis

Comparisons between mutant and control flies were made using Student's t test unless otherwise indicated; $p < 0.05$ was considered significant. All values plotted and written are means ± SEM.

### Acknowledgments

We thank Drs. Karen Palter, Seymour Benzer, Hugo Bellen, Erich Buchner, Regis Kelly, and Bing Zhang for antibodies or cDNAs, and Dr. Spyros Artavanis-Tsakonas and the Bloomington Stock Center for fly stocks. We also acknowledge Andrew Millar for his help with the Fura-2 measurements. This work has been supported by grants to K.E.Z. from the National Science Foundation (IBN-9604889), the National Institutes of Health (RO1NS38274), the March of Dimes Birth Defects Foundation, and the Whitehall Foundation, and by a National Research Service Award to P.B. (MH12611F31) from National Institute of Mental Health, and grants from the Medical Research Council of Canada to H.L.A.

Received September 14, 2000; revised March 27, 2001.

## References

Adams, M.D., Celniker, S.E., Holt, R.A., Evans, C.A., Gocayne, J.D., Amanatides, P.G., Scherer, S.E., Li, P.W., Hoskins, R.A., Galle, R.F., et al. (2000). The genome sequence of *Drosophila* melanogaster. Science *287*, 2185–2195.

Benfenati, F., Onofri, F., and Giovedi, S. (1999). Protein-protein interactions and protein modules in the control of neuroransmitter release. Phil. Trans. R. Soc. Lond. B. Biol. Sci. *354*, 243–257.

Betz, W.J., and Bewick, G.S. (1992). Optical analysis of synaptic vesicle recycling at the frog neuromuscular junction. Science *255*, 200–203.

Bollmann, J.H., Sakmann, B., and Borst, J.G. (2000). Calcium sensitivity of glutamate release in a calyx-type terminal. Science *289*, 953–957.

Braun, J., Wilbanks, S.M., and Scheller, R.H. (1996). The cysteine string secretory vesicle protein activates Hsc70 ATPase. J. Biol. Chem. *271*, 25989–25993.

Bukau, B., and Horwich, A.L. (1998). The Hsp70 and Hsp60 chaperone machines. Cell *92*, 351–366.

Capogna, M. (1998). Presynaptic facilitation of synaptic transmission in the hippocampus. Pharmacol. Ther. *77*, 203–223.

Ceccarelli, B., Hurlbut, W.P., and Mauro, A. (1973). Turnover of transmitter and synaptic vesicles at the frog neuromuscular junction. J. Cell Biol. *57*, 499–524.

Chamberlain, L.H., and Burgoyne, R.D. (1997). Activation of the ATPase activity of heat-shock proteins Hsc70/Hsp70 by cysteine-string protein. Biochem. J. *322*, 853–858.

Chamberlain, L.H., and Burgoyne, R.D. (2000). Cysteine String Protein: The Chaperone at the Synapse. J. Neurochem. *74*, 1781–1789.

Chang, H., Ciani, S., and Kidokoro, Y. (1994). Ion permeation properties of the glutamate receptor channel in cultured embryonic *Drosophila* myotubes. J. Physiol. *476*, 1–16.

Craig, E.A., Ingolia, T.D., and Manseau, L.J. (1983). Expression of *Drosophila* heat-shock cognate genes during heat shock and development. Develop. Biol. *99*, 418–426.

Cremona, O., and De Camilli, P. (1997). Synaptic vesicle endocytosis. Curr. Op. in Neurobiol. *7*, 323–330.

Dawson-Scully, K., Bronk, P., Atwood, H.L., and Zinsmaier, K.E. (2000). Cysteine-string protein increases the calcium sensitivity of neurotransmitter exocytosis in *Drosophila*. J. Neurosci. *20*, 6039–6047.

Debanne, D., Guerineau, N.C., Gahwiler, B.H., and Thompson, S.M. (1996). Paired-pulse facilitation and depression at unitary synapses in rat hippocampus: quantal fluctuation affects subsequent release. J. Physiol. *491*, 163–176.

Dodge, F.A., and Rahamimoff, R. (1967). Cooperative action of calcium ions in transmitter release at the neuromuscular junction. J. Physiol. *193*, 419–432.

Graham, M.E., and Burgoyne, R.D. (2000). Comparison of cysteine string protein (Csp) and mutant-SNAP overexpression reveals a role for Csp in late steps of membrane fusion in dense-core granule exocytosis in adrenal chromaffin cells. J. Neurosci. *20*, 1281–1289.

Greener, T., Grant, B., Zhang, Y., Wu, X., Greene, L.E., Hirsh, D., and Eisenberg, E. (2001). *Caenorabditis elegans* auxilin: a J-domain protein essential for clathrin-mediated endocytosis in vivo. Nat. Cell Biol. *3*, 215–219.

Gundersen, C.B., and Umbach, J.A. (1992). Suppression cloning of the cDNA for a candidate subunit of a presynaptic calcium channel. Neuron *9*, 527–537.

Heuser, J.E., and Reese, T.S. (1973). Evidence for recycling of synaptic vesicles at the frog neuromuscular junction. J. Cell Biol. *57*, 315–344.

Hing, H.K., Bangalore, L., Sun, X., and Artavanis-Tsakonas, S. (1999). Mutations in the heatshock cognate 70 protein (hsc4) modulate Notch signaling. Europ. J. Cell Biol. *78*, 690–697.

Jan, L.Y., and Jan, Y.N. (1976). Properties of the larval neuromuscular junction in *Drosophila melanogaster*. J. Physiol. (Lond.) *262*, 189–214.

Jiang, R., Gao, B., Prasad, K., Greene, L.E., and Eisenberg, E. (2000). Hsc70 chaperones clathrin and primes it to interact with vesicle membranes. J. Biol. Chem. *275*, 8439–8447.

Leveque, C., Pupier, S., Marqueze, B., Geslin, L., Kataoka, M., Takahashi, M., De Waard M., and Seagar, M. (1998). Interaction of cysteine string proteins with the alpha1A subunit of the P/Q-type calcium channel. J. Biol. Chem. *273*, 13488–13492.

Liu, G., and Tsien, R.W. (1995). Properties of synaptic transmission at single hippocampal synaptic boutons. Nature *375*, 404–408.

Magga, J.M., Jarvis, S.E., Arnot, M.I., Zamponi, G.W., and Braun, J.E.A. (2000). Cysteine string protein regulates G protein modulation of N-type calcium channels. Neuron *28*, 195–204.

Newmyer, S.L., and Schmid, S.L. (2001). Dominant-interfering Hsc70 mutants disrupt stages of the clathrin-coated vesicle cycle in vivo. J. Cell Biol. *152*, 607–620.

Nie, Z., Ranjan, R., Wenniger, J.J., Hong, S.N., Bronk, P., and Zinsmaier, K.E. (1999). Overexpression of cysteine string protein in *Drosophila* reveals interactions with syntaxin. J. Neurosci. *19*, 10270–10279.

Palter, K.B., Watanabe, M., Stinson, L., Mahowald, A.P., and Craig, E.A. (1986). Expression and localization of *Drosophila melanogaster* hsp70 cognate proteins. Mol. Cell. Biol. *6*, 1187–1203.

Perkins, L.A., Doctor, J.S., Zhang, K., Stinson, L., Perrimon, N., and Craig, E.A. (1990). Molecular and developmental characterization of the heat shock cognate 4 gene of *Drosophila melanogaster*. Mol. Cell. Biol. *10*, 3232–3238.

Ranjan, R., Bronk, P., and Zinsmaier, K.E. (1998). Cysteine string protein is required for calcium secretion coupling of evoked neurotransmission in *Drosophila* but not for vesicle recycling. J. Neurosci. *18*, 956–964.

Rorth, P., Szabo, K., Bailey, A., Laverty, T., Rehm, J., Rubin, G.M., Weigmann, K., Milan, M., Benes, V., Ansorge, W., and Cohen, S.M. (1998). Systematic gain-of-function genetics in *Drosophila*. Development *125*, 1049–1057.

Rothman, J.E., and Schmid, S.L. (1986). Enzymatic recycling of clathrin from coated vesicles. Cell *46*, 5–9.

Rubin, D.M., Mehta, A.D., Zhu, J., Shoham, S., Chen, X., Wells, Q.R., and Palter, K.B. (1993). Genomic structure and sequence analysis of *Drosophila melanogaster* HSC70 genes. Gene *128*, 155–163.

Schneggenburger, R., and Neher, E. (2000). Intracellular calcium dependence of transmitter release rates at a fast central synapse. Nature *406*, 889–893.

Spradling, A.C., Stern, D.M., Kiss, I., Roote, J., Laverty, T., and Rubin, G.M. (1995). Gene disruptions using P transposable elements: an integral component of the *Drosophila* genome project. Proc. Natl. Acad. Sci. USA *92*, 10824–10830.

Stewart, B.A., Atwood, H.L., Renger, J.J., Wang, J., and Wu, C.F. (1994). Improved stability of *Drosophila* larval neuromuscular preparations in haemolymph-like physiological solutions. J. Comp. Physiol. *175*, 179–191.

Takahashi, T., Hori, T., Kajikawa, Y., and Tsujimoto, T. (2000). The role of GTP-binding protein activity in fast central synaptic transmission. Science *289*, 460–463.

Umbach, J.A., and Gundersen, C.B. (1997). Evidence that cysteine string proteins regulate an early step in the $Ca^{2+}$-dependent secretion of neurotransmitter at *Drosophila* neuromuscular junctions. J. Neurosci. *17*, 7203–7209.

Umbach, J.A., Zinsmaier, K.E., Eberle, K.K., Buchner, E., Benzer, S., and Gundersen, C.B. (1994). Presynaptic dysfunction in *Drosophila* csp mutants. Neuron *13*, 899–907.

Ungewickell, E., Ungewickell, H., Holstein, S.E., Lindner, R., Prasad, K., Barouch, W., Martin, B., Greene, L.E., and Eisenberg, E. (1995). Role of auxilin in uncoating clathrin-coated vesicles. Nature *378*, 632–635.

Wu, M.N., Fergestad, T., Lloyd, T.E., He, Y., Broadie, K., and Bellen, H.J. (1999). Syntaxin 1A interacts with multiple exocytic proteins to regulate neurotransmitter release in vivo. Neuron *23*, 593–605.

Yuan, L., and Ganetzky, B. (1999). A glial-neuronal signaling pathway revealed by mutations in a neurexin-related protein. Science *283*, 1343–1345.

Zinsmaier, K.E., Eberle, K.K., Buchner, E., Walter, N., and Benzer, S. (1994). Paralysis and early death in cysteine string protein mutants of *Drosophila*. Science *263*, 977–980.

Zinsmaier, K.E., Hofbauer, A., Heimbeck, G., Pflugfelder, G.O., Buchner, S., and Buchner, E. (1990). A cysteine-string protein is expressed in retina and brain of *Drosophila*. J. Neurogenet. *7*, 15–29.

Zucker, R.S. (1989). Short-Term Synaptic Plasticity. Ann. Rev. Neurosci. *12*, 13–31.